Interaction of the C-Terminal Region of the Gγ Protein with Model Membranes

Francisca Barceló,* Jesús Prades,* José Antonio Encinar,† Sérgio S. Funari,‡ Oliver Vögler,* José Manuel González-Ros,† and Pablo V. Escribá*

*Laboratory of Molecular and Cellular Biomedicine, Associate Unit of the Instituto de la Grasa (Consejo Superior de Investigaciones Científicas), University of the Balearic Islands, E-07122 Palma de Mallorca, Spain; †Instituto de Biología Molecular y Celular, Universidad Miguel Hernández, E-03206 Elche, Spain; and ‡Hamburger Synchrotronstrahlungslabor, D-22603 Hamburg, Germany

ABSTRACT Heterotrimeric G-proteins interact with membranes. They accumulate around membrane receptors and propagate messages to effectors localized in different cellular compartments. G-protein-lipid interactions regulate G-protein cellular localization and activity. Although we recently found that the G$\beta\gamma$ dimer drives the interaction of G-proteins with nonlamellar-prone membranes, little is known about the molecular basis of this interaction. Here, we investigated the interaction of the C-terminus of the Gγ_2 protein (P_γ-FN) with model membranes and those of its peptide (P_γ) and farnesyl (FN) moieties alone. X-ray diffraction and differential scanning calorimetry demonstrated that P_γ-FN, segregated into P_γ-FN-poor and -rich domains in phosphatidylethanolamine (PE) and phosphatidylserine (PS) membranes. In PE membranes, FN increased the nonlamellar phase propensity. Fourier transform infrared spectroscopy experiments showed that P_γ and P_γ-FN interact with the polar and interfacial regions of PE and PS bilayers. The binding of P_γ-FN to model membranes is due to the FN group and positively charged amino acids near this lipid. On the other hand, membrane lipids partially altered P_γ-FN structure, in turn increasing the fluidity of PS membranes. These data highlight the relevance of the interaction of the C-terminal region of the Gγ protein with the cell membrane and its effect on membrane structure.

INTRODUCTION

G-protein-coupled receptors (GPCRs) constitute the largest gene family known in humans. These receptors are involved in many relevant cellular and physiological processes (e.g., the control of blood pressure, cellular proliferation, and body weight), and the messages they receive are propagated and amplified through G-proteins. In this signal-transduction process, G-proteins shuttle from the cytosol to the membrane and vice versa assisted by co/posttranslational lipid modifications, such as a farnesyl (FN) moiety in the C-terminal region of the Gγ subunit (1,2). Lipid modifications might also be involved in i), the recruitment of heterotrimeric (G$\alpha\beta\gamma$) proteins to GPCR-rich regions, and ii), the segregation of the Gα subunit from the G$\beta\gamma$ complex and their localization to different membrane regions upon receptor activation by agonists. For this reason, it is not possible to fully understand G-protein function without a comprehensive knowledge of their interaction with membrane lipids.

The cytosolic monolayer of the plasma membrane is formed mainly by phosphatidylethanolamine (PE) and phosphatidylserine (PS). We have studied the interaction of the C-terminal region of the Gγ_2 protein subunit with model membranes formed of these lipids. The prenyl moiety of the γ-subunit seems to be relevant in both protein-protein and lipid-lipid interactions (2–13). Nevertheless, its role in the interaction between G-proteins and membranes and its influence on membrane structure remain unclear (9,14,15). It has been suggested that the hydrophobic isoprenyl group attached to the γ-subunit of the G$\beta\gamma$ complex could affect the membrane docking of G-proteins (10,11). On the other hand, G-protein-membrane interaction is also regulated by the physical properties of the lipid bilayer (16).

We have already shown that heterotrimeric G$\alpha\beta\gamma$ proteins and G$\beta\gamma$ dimers bind more readily to nonlamellar (H_{II}) prone membrane regions than to lamellar-prone bilayers (9,17). Moreover, the G$\beta\gamma$ dimer drives the interaction of heterotrimeric Gi proteins with membranes containing high levels of PE (i.e., with a high nonlamellar phase propensity), such as the inner leaflet of the cell membrane (9). Since the Gβ subunit does not appear to be relevant in this interaction (10), the Gγ subunit could account for the binding of G-proteins to membrane domains with high H_{II} phase propensity. In addition, the G$\beta\gamma$ dimer binds strongly to membranes formed by PS lipids (18–20). Besides the lipid modification (e.g., FN) found in G-protein γ-subunits, its C-terminal also contains cationic amino acids that might participate in electrostatic interactions between G-proteins and PS membrane (20).

We therefore investigated the interaction of the C-terminal region of Gγ_2 protein with model membranes composed of the major phospholipids (PE and PS) found at the inner leaflet of the plasma membrane to study its role in the interaction between G-proteins and lipid bilayers. For this purpose, we used both the farnesylated (P_γ-FN) and nonfarnesylated (P_γ)

Submitted November 15, 2006, and accepted for publication March 19, 2007.

Address reprint requests to Francisca Barceló, Depto. de Biología Fundamental, University of the Balearic Islands, E-07122 Palma de Mallorca, Spain. Tel.: 349-7117-3149; Fax: 439-7117-3184; E-mail: francisca.barcelo@uib.es.

Editor: Paul H. Axelsen.

0006-3495/07/10/2530/12 $2.00

doi: 10.1529/biophysj.106.101196

peptides from the C-terminal amino acid region of the bovine $G\gamma_2$ subunit (Swiss-Prot: P63212) as well as the isolated nonpeptide FN moiety. The results presented here in part explain the molecular bases underlying the interaction of G-proteins with membranes, which to date were largely unknown and the cooperative binding of G-proteins to membranes necessary to amplify GPCR signals.

MATERIALS AND METHODS

Materials

1,2-dielaidoyl-*sn*-glycero-3-phosphoethanolamine (DEPE), 1,2-dimyristoyl-*sn*-glycero-3-phosphate sodium salt (DMPA), and 1,2-dimyristoyl-*sn*-glycero-3-phosphatidylserine (DMPS) were purchased from Avanti Polar Lipids (Alabaster, AL). They were stored under argon at −80°C. 1-(4-Trimethylammoniumphenyl)-6-phenyl-1,3,5-hexatriene *p*-toluenesulfonate (TMA-DPH) and 1-hexadecanoyl-2-(1-pyrenedecanoyl)-*sn*-glycero-3-phosphoethanolamine (HPE) were obtained from Molecular Probes (Eugene, OR). Hepes and D_2O were obtained from Sigma Chemical (Poole, Dorset, UK).

Peptide synthesis and characterization

Two peptides were synthesized at the University of Barcelona (Barcelona, Spain). One corresponded to the nonfarnesylated C-terminal region (amino acid sequence 48–70) of the bovine $G\gamma_2$ subunit (Swiss-Prot: P63212): PLLTPVPASENPFREKKFFCAIL-amide (P_γ). It was synthesized as a carboxy-terminal amide on an automatic peptide synthesizer (Abi 430A, Applied Biosystems, Foster City, CA). The second (farnesylated) peptide contained the same amino acid sequence, but it was prepared with an all-*trans*-FN group linked to the cysteine residue through a thioether linkage: PLLTPVPASENPFREKKFFC[FN]AIL-amide (P_γ-FN). The farnesylation method was essentially that described previously (21). Both peptides were purified to 95% purity by reverse-phase high performance liquid chromatography and further analyzed by amino acid analysis matrix-assisted laser desorption ionization-time of flight mass spectrometry. Residual trifluoroacetic acid from peptide purification was removed by three lyophilization-solubilization cycles in 10 mM HCl to avoid interference in the characterization of the amide I′ band in Fourier transform infrared (FTIR) spectroscopy studies (22). Due to the different water solubility of the peptides, stock solutions of P_γ-FN and P_γ were prepared in chloroform/methanol and Hepes buffer, respectively, and were stored at −80°C until use.

Model membranes and sample preparation

For x-ray diffraction experiments, multilamellar lipid vesicles (MLV) containing 15% (w/w) lipids in aqueous solution were prepared in 10 mM Hepes, 100 mM NaCl, 1 mM EDTA, pH 7.4 (Hepes buffer) according to established procedures (23). Lipid powder was hydrated in the presence or absence of P_γ-FN or P_γ at the desired molar ratio, and the mixture was thoroughly homogenized with a pestle-type minihomogenizer (Sigma Chemical) and by vortexing. The suspensions were then submitted to five temperature cycles (heating to 70°C and cooling to 4°C) and equilibrated before data acquisition.

For differential scanning calorimetry (DSC) and fluorescence spectroscopy experiments, MLV were prepared from the membranes using a similar protocol. The lipids were dissolved in chloroform/methanol (2:1, v/v), and the solvent was evaporated under argon and vacuum dried to obtain a lipid film. The film was hydrated by addition of Hepes buffer to a final concentration of 15% (w/w), and the mixtures were submitted to five temperature cycles (60°C and 4°C) to ensure complete homogenization. For fluorescence spectroscopy experiments, lipids and TMA-DPH (lipid/probe, 200:1, mol/mol), were dissolved together in chloroform/methanol (2:1, v/v). The film obtained was hydrated to a final lipid concentration of 25–30 μM. Small unilamellar vesicles (SUV) only were used for fluorescence experiments. They were prepared from MLV by sonication in an ice water bath with a Branson 250 sonicator (Branson, Danbury, CT) equipped with a microtip until the solution became clear.

For infrared amide I′ band recordings from peptide samples, aliquots of P_γ-FN stock solution (~225 μg) were evaporated under argon and vacuum dried. The peptide powder was resuspended in D_2O-Hepes buffer (pH 7.4) to avoid interference of the H_2O infrared absorbance (1645 cm^{-1}). Alternatively, aliquots of P_γ in Hepes buffer were dried in a speed-vac Savant rotary evaporator (Farmingdale, NY) and resuspended in D_2O to obtain a D_2O buffer with identical saline composition as in H_2O. For FTIR studies, lipid vesicles were prepared as described above except that the lipid film was hydrated by adding D_2O-Hepes buffer (pH 7.4). Peptide samples reconstituted into lipid vesicles were prepared by two different procedures depending on the water solubility of the peptide used. First, aliquots of P_γ-FN and lipids solutions were mixed to obtain the desired lipid/peptide molar ratio. The solvent was evaporated under argon and vacuum dried. These powdered lipid/peptide mixtures were then hydrated by adding D_2O-Hepes buffer (pH 7.4). Second, aliquots of P_γ samples were added directly to the lipid dispersion prepared in Hepes buffer at the final lipid/peptide molar ratio. The mixtures were lyophilized and then resuspended in D_2O. In both procedures, lipid/peptide samples were heated to 60°C, submitted to vortex shaking, and cooled down to 4°C. This cycle was repeated five times to obtain a homogeneous dispersion. For infrared phosphate stretching band recordings, lipid vesicles were prepared in the presence or absence of peptide as described above, except that they were hydrated in Hepes buffer (pH 7.4).

X-ray diffraction analysis

Small and wide-angle synchrotron radiation x-ray scattering (SAXS and WAXS) data were collected simultaneously, using standard procedures on the Soft Condensed Matter beamline A2 of HASYLAB of the Deutsches Elektronen Synchrotron (DESY). Samples were heated from 27°C to 75°C and then cooled down to 27°C at a scan rate of 1°C/min. For the measurement of the samples in quasiequilibrium conditions, the lipid mixtures were allowed to equilibrate for 15 min at each temperature before taking measurements. The data collection conditions were the same as those described previously (23).

Differential scanning calorimetry

Experiments were carried out on a high-resolution differential scanning microcalorimeter (MC-2; Microcal, Studio City, CA). MLV obtained from DEPE and DMPS (2 mM in lipid phosphorus) in the absence or presence of the P_γ-FN or P_γ peptide or FN were heated at a scan rate of 1°C/min. Transition temperatures and enthalpies were calculated by fitting the transitions to a single Van't Hoff component. The deconvolution analysis of the calorimetric peaks was performed using the software provided by the manufacturer. The lipid phase transition temperatures (T_m and T_H) corresponded to the maximum excess heat capacity.

FTIR spectroscopy

Sample measurements were performed in a liquid demountable cell (Harrick, Ossining, NY) equipped with CaF_2 windows and 50-μm-thick Mylar spacers. These were maintained at 20°C for 30 min to ensure the temperature equilibration of the sample. FTIR analysis was carried out on Bruker (Billerica, MA) IFS 66/S and Nicolet (Madison, WI) 520 instruments equipped with deuterated tryglycine sulfate detectors. The sample chamber was constantly purged with dry air. A minimum of 75 scans per spectra was taken, averaged, apodized with a Happ-Genzel function, and Fourier

transformed to give a nominal resolution of 2 cm^{-1}. Self-deconvolution was performed using a Lorenztian bandwidth of 12 cm^{-1} and a resolution enhancement factor of 1.8. The temperature scan was from 25°C to 60°C for DMPS and DMPA and from 30°C to 75°C for DEPE, measured in steps of 2°C. Afterward, the samples were cooled and equilibrated at 20°C to check the reversibility of the transitions.

Peptide-membrane interactions were studied using MLV in D_2O-Hepes buffer (45 mM in lipid phosphorus) at lipid/peptide ratios of 20:1, 10:1, and 5:1. The membrane-bound peptide was separated from the free peptide by centrifugation at 20,000 × *g* for 20 min at 4°C. The pellets were resuspended in 20 μL of D_2O-Hepes buffer. The amide I′ band region of these samples and that of the supernatants were further analyzed.

Fluorescence polarization spectroscopy

Experiments were carried out on a thermostated Perkin-Elmer MPF-66 fluorescence spectrophotometer (Foster City, CA). SUV containing phospholipids, peptide, and the fluorophore TMA-DPH were excited at 360 nm, and emission was registered at 427 nm, with bandwidths of 4 nm. Samples were equilibrated for 5 min at each temperature before measurement. In our experimental conditions, the inner filter effect became critical when sample absorption was ~0.1 (24). Therefore, lipid samples were diluted to a concentration of ~25 μM for DEPE and 50 μM for DMPS. Under these conditions, the samples had absorptions of ~0.095 for DEPE and 0.05 for DMPS at the excitation wavelength used. Light scattering was always checked using unlabeled liposomes. Fluorescence intensity from samples without fluorophore was <1% for DMPS and <30% for DEPE. In DEPE mixtures, the contribution of scattered light from the excitation source to the measured light at 427 nm was not negligible. Both the parameters of intensity and polarization were affected by the scattered light. For this reason, the scattered light intensity and polarization were determined by measuring unlabeled control samples in the same conditions as labeled mixtures. We used the corrections for the scattered light contribution (fluorescence intensity and polarization measurements) described elsewhere (25). Fluorescence polarization was calculated according to the equation (26)

$$P = (I_{VV} - GI_{VH})/(I_{VV} + GI_{VH}),$$

where I_{vv} and I_{vh} are the fluorescence intensity values measured with the excitation and emission polarizers in parallel and perpendicular, respectively, and G is the instrumental factor. All fluorescence polarization data are mean values from three independent experiments.

RESULTS

Peptide structure and peptide-membrane association

P_γ-FN and P_γ exhibited an amide I′ band (Fig. 1, *A* and *D*) characteristic of β-sheet structures with maxima at 1625 (P_γ-FN) or 1638 (P_γ) cm^{-1} and a weak component at around 1688 cm^{-1} (27). Amide I′ spectra of both peptides also displayed a random-coil component with a prominent shoulder around 1645–1649 cm^{-1} (28). These structures were stable in the temperature range studied.

We used a centrifugation assay to qualitatively analyze the membrane binding of both peptides under the conditions used in FTIR experiments (Fig. 1, *B*, *C*, *E*, and *F*). We found binding of P_γ-FN to DEPE and DMPA membranes, as the amide I′ band appeared exclusively in the membrane pellet and not in the aqueous phase (supernatant). In addition, the band at 1625 cm^{-1} was more prominent in the presence of DEPE and even more so in the presence of DMPA (Fig. 1, *B* and *C*). Both properties could indicate an increase in the proportion of P_γ-FN that adopts a β-sheet structure as a result of its association with DEPE or DMPA lipids. In principle, such a β-structure could either be intramolecular or intermolecular. Additional experiments using different peptide concentrations and different protein/lipid ratios result in different 1625:1645 absorbance ratios (data not shown), thus, supporting the idea that intermolecular structures might be formed as a result of a concentration-dependant oligomerization process.

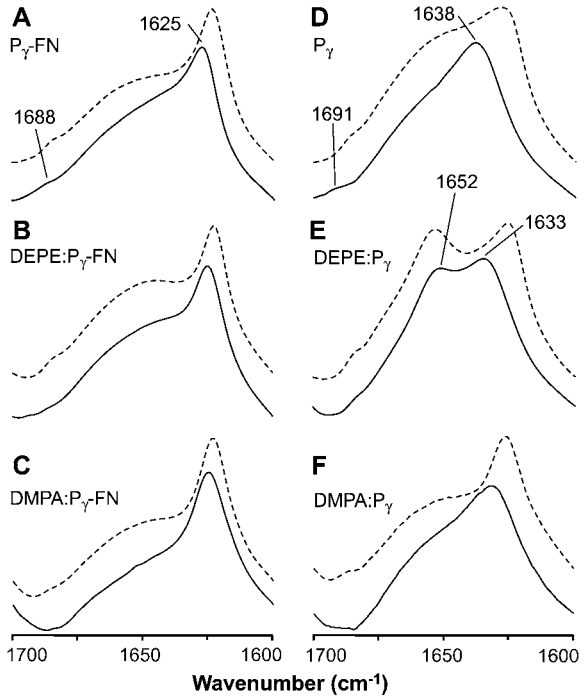

FIGURE 1 FTIR amide I′ band region spectra of P_γ-FN and P_γ peptides. (*A* and *D*) Pure peptides and (*B*, *C*, *E*, and *F*) pellets of DEPE- or DMPA-peptide mixtures centrifugated and resuspended in Hepes buffer prepared with D_2O. The lipid/peptide molar ratio was 10:1 in all cases. The buffer spectrum was subtracted from those of the samples containing the peptides. The traces shown in each plot correspond to the spectra acquired at 20°C (——) and 55°C (- - - -).

In the case of the P_γ peptide and in the presence of DMPA membranes, we only observed the amide I′ band in the membrane pellet similarly to that found above for the P_γ-FN peptide. Conversely, the P_γ peptide in DEPE membranes shows amide I′ bands in both the membrane pellet and the aqueous supernatant, indicating that there was only partial association of the peptide with DEPE membranes. Additionally, the spectra of P_γ in DEPE membranes showed two main bands at ~1652 cm^{-1} and 1633 cm^{-1}, which clearly differed from the FTIR spectrum of P_γ alone. This might indicate that the association of the peptide with DEPE bilayers induces a partial loss of the β-sheet secondary structure, adopting α-helical and/or random coil structures (29).

DMPS has the asymmetric stretching carboxyl group band of the serine moiety [$\nu_{as}(COO^-)$] around 1628–1640 cm^{-1}, so that the amide I′ region shows certain overlap with this band (30), making it very difficult to characterize DMPS-peptide interactions using this technique.

Structural influence of the peptides on the supramolecular organization of DEPE and DMPS membranes

DEPE and DMPS, widely used as models of biological membranes, were chosen because they belong to the most abundant lipid classes of the inner leaflet of the plasma membrane. In this context, the melting temperatures for them (30°C–40°C) and the lamellar-to-hexagonal (H_{II}) phase transition temperature of DEPE (60°C–70°C) are compatible with all the techniques used, whereas other synthetic or natural phosphatidyl-ethanolamine/serine have transition temperatures that hamper the application of some of the experimental approaches used in this study.

X-ray diffraction analysis permitted the structural properties of DEPE- and DMPS-peptide mixtures to be characterized (Fig. 2). It is noteworthy that DEPE/P_γ-FN mixtures showed a complex x-ray diffraction pattern that was further studied under quasiequilibrium conditions (Fig. 2, *A*, *B*, *E*). The mesomorphic behavior of DEPE was similar to that described previously (23,24). DEPE, DEPE/P_γ-FN, and DEPE/P_γ mixtures showed a phase sequence from gel lamellar phase (L_β) to liquid crystalline lamellar phase (L_α) and then to H_{II} as the temperature increased (Fig. 2 *D*). The temperature range for the L_α-to-H_{II} phase transition depended on the peptide concentration, whereas the structural parameters were scarcely affected (Table 1). P_γ peptide stabilized the coexistence of the L_α phase with the H_{II} phase up to 71°C ($d \sim 6.6$ nm). In contrast, P_γ-FN exerted a modest effect on the lamellar phase.

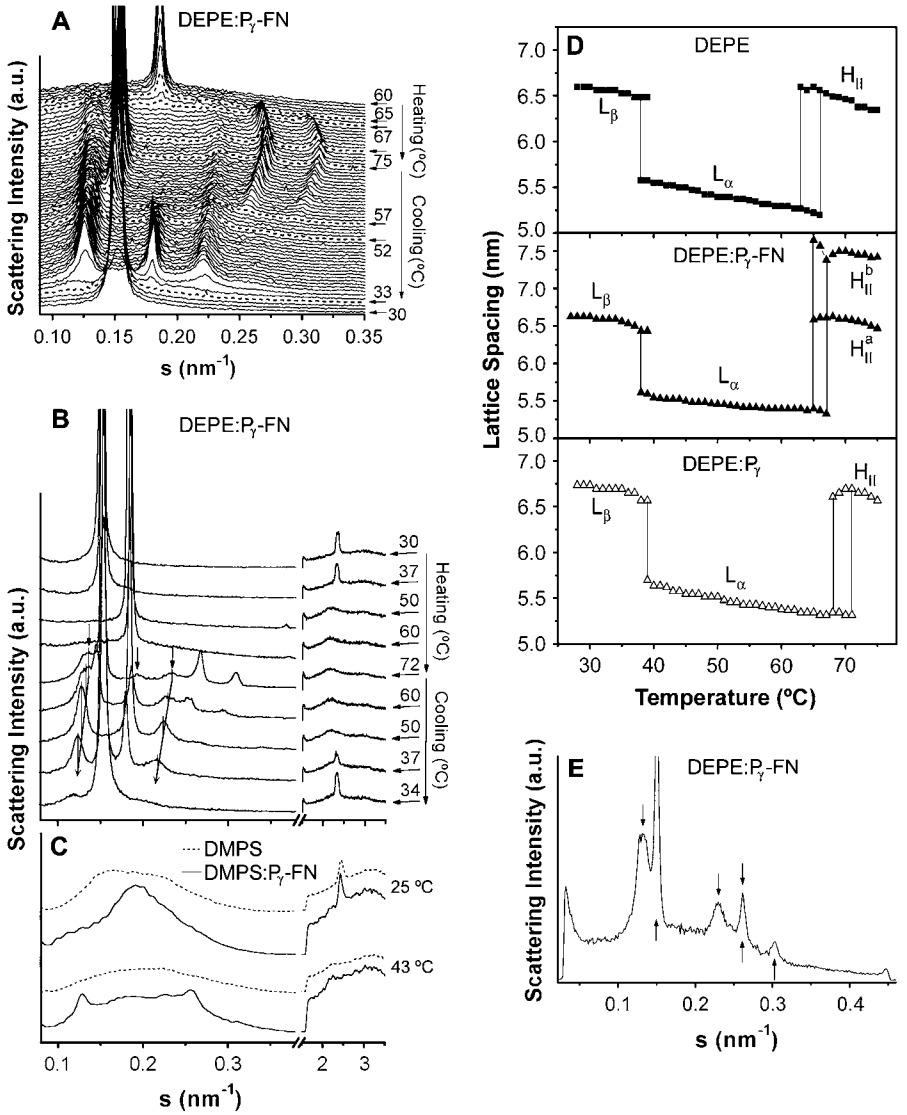

FIGURE 2 Linear plots of the x-ray scattering patterns of DEPE/P_γ-FN and DMPS/P_γ-FN mixtures. (*A* and *B*) DEPE/P_γ-FN (20:1, mol/mol) and (*C*) DMPS/P_γ-FN (10:1, mol/mol) samples. The sequence of the patterns were acquired under (*A*) kinetic conditions with a scan rate of 1°C/min and (*B* and *C*) quasiequilibrium conditions, after equilibrating the sample during 15 min at each temperature. Successive diffraction patterns were collected for 15 s each minute. The L_β-to-L_α phase transition was identified by the disappearance of the peak in the WAXS region. (*D*) The dependence of lattice spacing on the temperature for DEPE alone and in the presence of P_γ-FN or P_γ at a 10:1 (DEPE/peptide) molar ratio. The phases represented are L_β, L_α, and H_{II}. The coexistence of L_α and H_{II} phases corresponds to the temperature range defined by the vertical lines. Only the heating sequence from 27°C to 75°C is shown here. (*E*) Diffraction pattern of DEPE/P_γ-FN sample at 63°C. The arrows indicate the diffractions' peaks corresponding to the two hexagonal phases with an epitaxial relationship.

TABLE 1 Structural properties of DEPE membranes containing the C-terminal Gγ peptide

Sample	Molar ratio	$\delta d/\delta T$ (*L_β) (nm/°C)	$\delta d/\delta T$ (*L_α) (nm/°C)	$\delta d/\delta T$ (*H_{II}) (nm/°C)	†$\Delta T_{L\alpha}$/°C	‡$d_{L\beta}$ (nm)	†$d_{L\alpha}$ (nm)	†d_{HII} (nm)
DEPE	1:0	−0.012	−0.013	−0.023	(38)39–63(66)	6.59	5.55	6.40
DEPE/P_γ	10:1	−0.015	−0.011	–	39–68(71)	6.73	5.64	6.65
DEPE/$P_{\gamma\text{-FN}}$	40:1	−0.010	−0.009	−0.019	(38)39–64(66)	6.59	5.57	6.52
DEPE/$P_{\gamma\text{-FN}}$	20:1	−0.002	−0.007	−0.021	(38)39–65(67)	6.62	5.54	6.56
		–	–	−0.015§	66§(67)	–	–	7.45§
DEPE/$P_{\gamma\text{-FN}}$	10:1	−0.004	−0.009	−0.024	40–67(69) 68	6.68	5.67	6.70
		–	–	–	(69)§	–	–	7.57§
DEPE/FN	40:1	−0.009	−0.011	−0.024	(36)38–54(61)	6.57	5.46	6.26

$P_{\gamma\text{-FN}}$ and P_γ are the farnesylated and nonfarnesylated peptides, respectively. The angular coefficient of the dependence of the lattice spacing on temperature $\delta d/\delta T < 0$ indicates a compression process.

*The compressibility of the phase is linear in the single or two-phase regions.

†The temperature range where the L_α phase is observed is shown, $\Delta T_{L\alpha}$. The brackets indicate the temperature limit of the L_α phase in a two-phase region. Values on the left corresponds to the $L_\beta + L_\alpha$ and on the right to the $L_\alpha + H_{II}$ temperature range of phase coexistence. Lattice spacing,

‡$d_{L\beta}$ at 30°C, $d_{L\alpha}$ at 40°C, and d_{HII} at 72°C.

§Structural properties of the second nonlamellar H_{II} phase (H_{II}†).

Two sets of diffraction peaks were obtained from DEPE membranes in the presence of P_γ-FN within the temperature range of the H_{II} phase (Fig. 2, *A*, *B*, *E*). In the first, three narrow peaks were assigned to an inverted hexagonal phase (H_{II}^a) with lattice spacing $d = 6.5$ nm at 72°C. These peaks represent an almost pure lipid phase (little peptide is present). Their positions were affected by temperature corresponding to a contraction on heating and reversible expansion on cooling. The second set involved a series of two broad peaks assigned to first- and second-order reflections of a second inverted hexagonal phase (H_{II}^b), with $d = 7.4$ nm. These peaks were associated with a peptide-rich phase, and they were hardly affected by the temperature. In the cooling process, the nonlamellar phases coexisted up to a temperature of 52°C. During this process, the larger hexagonal phase (H_{II}^b) remained basically unchanged, whereas the smaller one (H_{II}^a) expanded almost linearly until both merged. Simultaneously, it is observed that the onset of the L_α phase ($s = 1/d = 0.18$ nm^{-1}) at 57°C and a strong decrease in the contribution from the smaller H_{II}^a phase, with only reminiscent peaks (see Fig. 2 *A*). Cooling further, a transition to a single L_β phase occurred at 35°C. Interestingly, these two hexagonal phases are epitaxially related by the planes [200] of the larger structure and [110] of the smaller one presenting the same interplanar distance ($s = 0.26$ nm^{-1} at 63°C) (Fig. 2 *E*). Other possible symmetries, e.g., cubic, were dismissed because the peak profiles were clearly divided into two groups, each matching an H_{II} phase structure. Indeed, when compiled together, they did not fit other common structures formed by self-assembled lipid.

The thermotropic behavior of DMPS was characterized by a sharp peak in the WAXS region that allowed the identification of the L_β phase at 25°C, which vanished when the temperature increased. In the presence of P_γ-FN, DMPS showed three broad diffraction peaks in the SAXS region (at 43°C) that were not present in pure DMPS, indicating that the presence of the farnesylated peptide induced some degree of structural order in the lipid bilayer organization (Fig. 2 *C*).

Differential scanning calorimetry

The thermotropic behavior of DEPE- and DMPS-peptide or −FN mixtures was further studied by differential scanning calorimetry (DSC) (Fig. 3). DEPE showed two phase transitions corresponding to the L_β-to-L_α phase transition ($T_m = 37.1$°C and enthalpy = 7.2 kcal/mol) and to the L_α-to-H_{II} phase transition ($T_H = 65$°C and enthalpy = 0.6 kcal/mol) (Fig. 3, *A* and *B*). The presence of P_γ-FN did not affect the T_m and slightly decreased the enthalpy associated with the L_β-to-L_α phase transition. The main effect of P_γ-FN on the thermotropic behavior of DEPE was a concentration-dependent decrease in the enthalpy and a broadening of the peak associated with the L_α-to-H_{II} transition and the T_H value was virtually unaffected. In contrast, FN alone induced the splitting of the L_β-to-L_α phase transition into two peaks and decreased the T_H value and the cooperativity of the L_α-to-H_{II} transition, as previously reported (31). On the other hand, P_γ increased the melting temperature of both L_β-to-L_α and L_α-to-H_{II} phase transitions.

Working with DMPS/P_γ-FN mixtures, P_γ-FN induced the splitting of the DMPS calorimetric peak associated to L_β-to-L_α phase transition into two separate peaks (Fig. 3 *C*). The shift in the maximum excess heat capacity of the first peak and the relative area of the two peaks were dependent on the concentration of P_γ-FN (Fig. 3 *D*). The transition temperature and cooperativity of the second peak was relatively insensitive to peptide concentration and closely resembled the DSC endotherm of DMPS alone ($T_m = 36.3$°C). Moreover, the transition enthalpy decreased in a peptide concentration-dependent manner. In turn, FN induced a progressive and significant reduction of the phase transition of DMPS with a decrease in the cooperativity and the enthalpy.

Study of peptide-lipid interactions by FTIR

We studied the molecular basis of the interactions of P_γ-FN, P_γ, and FN with zwitterionic and anionic phospholipids.

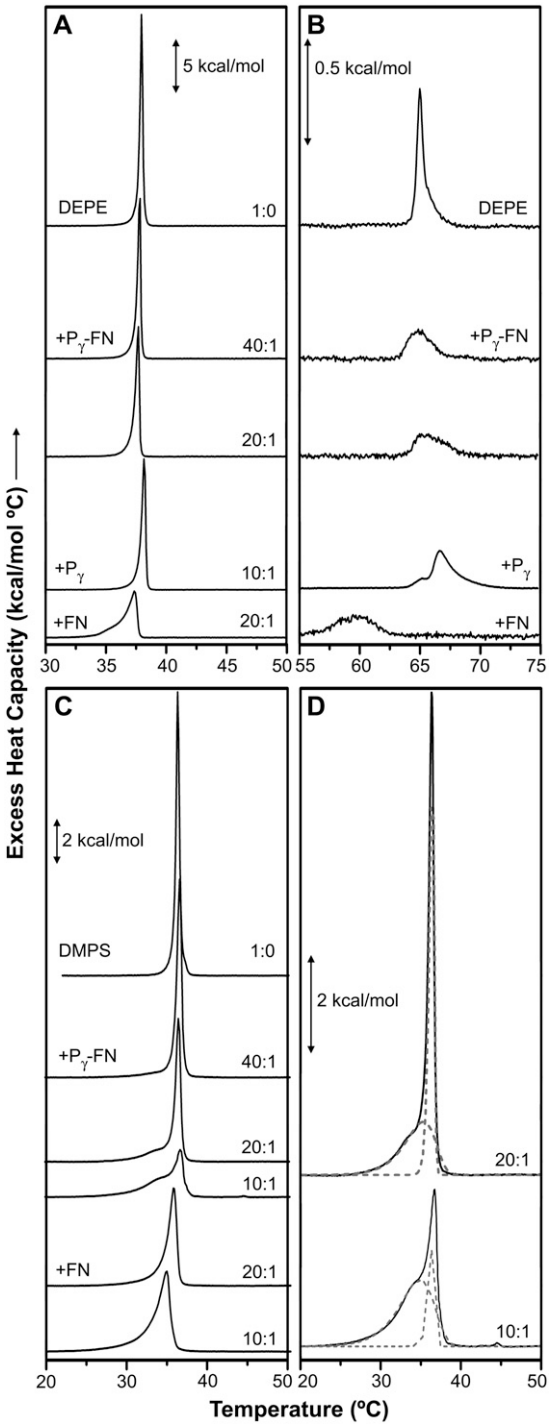

FIGURE 3 DSC thermograms of DEPE- or DMPS-peptide mixtures. (*A*), (*B*) DEPE, and (*C*) DMPS alone and in the presence of P_γ-FN, P_γ, or FN. The molar ratio of the mixtures is indicated by each thermogram. DSC scans were performed at a scan rate of 1°C/min. (*D*) Deconvolution analysis of the calorimetric peak: experimental data (——) and individual components (- - -) of DMPS/P_γ-FN mixtures at the molar ratio specified.

Specifically, we analyzed the phosphate-, carbonyl-, and methylene-stretching mode regions of the infrared spectra. The first was evaluated using DMPA membranes and the last with DEPE and DMPS vesicles.

Membrane lipid polar region

The spectral characteristics of the phosphate spectral region of DMPA in the presence and absence of P_γ-FN or P_γ were similar in L_β (25°C) and L_α (60°C) (Fig. 4). Both peptides affected the profile of the phospholipid phosphate vibrations in a concentration-dependent manner. The antisymmetric and symmetric stretching modes of the PO_2^- groups appeared at 1180 and 1085 cm^{-1}, respectively. P_γ-FN and P_γ induced shifts of these bands toward lower frequencies (~1170 and 1065 cm^{-1}, respectively). The antisymmetric and symmetric stretching modes of the PO_2^{2-} groups were also observed at 1100 and 985 cm^{-1}, respectively (32). Indeed, both peptides

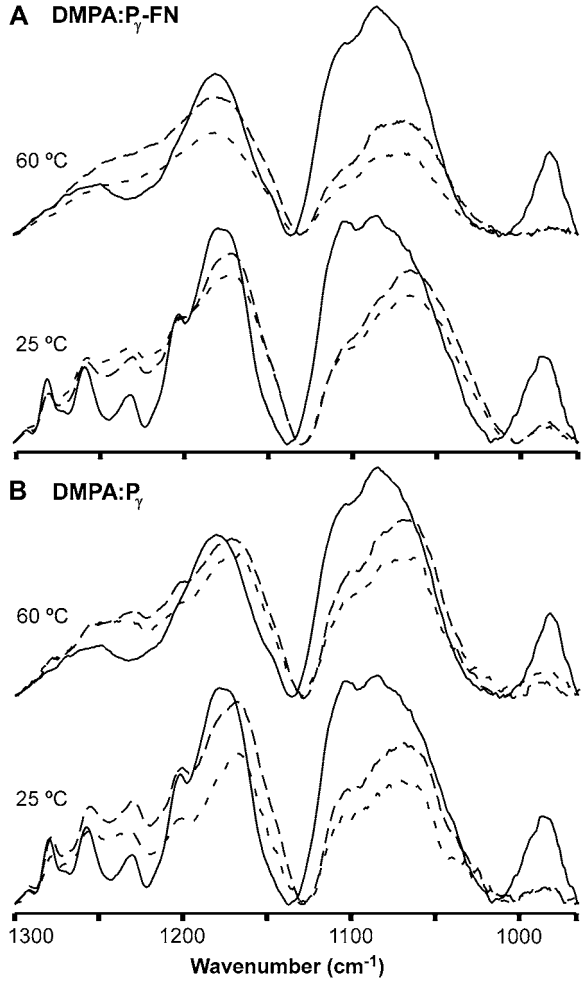

FIGURE 4 FTIR spectra of the phosphate stretching mode region of DMPA-peptide mixtures. DMPA alone (——) and in the presence of (*A*) P_γ-FN or (*B*) P_γ peptides. The lipid/peptide molar ratios were 10:1 (– – –) and 5:1 (- - -). The samples were prepared in aqueous Hepes buffer and measured at 25°C and 60°C.

decreased the spectral signals of the PO_2^{2-} group, and the band at 1100 cm^{-1} was slightly shifted toward a lower frequency, indicating a neutralization of the PO_2^{2-} group in the presence of P_γ-FN or P_γ (33). The presence of FN alone, at FN/phospholipid ratios up to 1:10, does not result in significant alteration of this phosphate spectral region. These results suggest that both peptides interact with the headgroup of acidic phospholipids, highlighting the relevant role of the amino acid moiety of the C-terminal region of Gγ subunits in the interaction of G-proteins with negatively charged membrane lipids.

Membrane lipid interfacial region

Self-deconvolution reveals two bands observed in the carbonyl stretching region at 1740 and 1720 cm^{-1} for DEPE (Fig. 5 *A*) and at 1740 and 1730 cm^{-1} for DMPS (Fig. 5 *B*), in agreement with earlier data (34,35). The low-frequency (~1720 or 1730 cm^{-1}) and the high-frequency (~1740 cm^{-1}) components of these spectra were attributed to hydrogen and nonhydrogen bonds between the phospholipid carbonyl group and water, respectively (36). The temperature-dependent changes in the h_{1740}/h_{1720} DEPE and h_{1740}/h_{1730} DMPS band ratios were analyzed in the presence or absence of P_γ-FN, P_γ, or FN. In DEPE membranes (Fig. 5 *C*), the differential effect of P_γ-FN and P_γ on the intensity band ratio h_{1740}/h_{1720} was notable in the L_β and L_α phases. In contrast to FN, both peptides produced a strong increase in the band ratio due to the dehydration of the carbonyl groups. For example, the I_{1740}/I_{1720} increased from ~1.6 in DEPE alone to 3.0–4.0 in the DEPE/peptide mixture at 30°C. These spectral changes can be attributed to the interaction of the peptide group with carbonyl groups from DEPE at the membrane interface. Such effects were much smaller when either DMPS or DMPA membranes were used in the studies. For instance, Fig. 5 *D* shows experiments with DMPS membranes in which P_γ-FN (more than P_γ and FN) decreased the intensity of the h_{1740}/h_{1730} band ratio from ~1.3 for the DMPS membranes alone only to ~1.2 for DMPS/P_γ-FN mixtures.

Phospholipid acyl chain region

We studied the thermal dependence of the methylene symmetric stretching mode ($\nu_s(CH_2)$) around 2850 cm^{-1} in the DEPE and DMPS mixtures (Fig. 6). The frequency of this band was sensitive to the conformational order of the acyl chain and to the *trans-gauche* isomerization of the lipids (37–39). The L_β-to-L_α phase transition occurred at 38°C and 40°C for DEPE and DMPS, respectively, as revealed by a 2 cm^{-1} band shift. In DEPE membranes (Fig. 6 *A*), P_γ-FN and P_γ reduced the conformational order in the bilayer core for both the L_β and L_α phases as a result of the formation of additional gauche rotamers (37). We were limited to analyzing the L_α-to-H_{II} phase transition temperature of DEPE/peptide mixtures by spectroscopy. In turn, DEPE/FN mixtures followed a particular trend that was characterized in a previous study (31). On the other hand, P_γ-FN and P_γ induced similar effects on the temperature-dependent shift of the 2850 cm^{-1} band in DMPS bilayers (Fig. 6 *B*), which differed from those of membranes formed exclusively by lipids (DMPS in the presence or absence of FN). Both peptides increased the acyl chain order in the L_α phase, slightly lowered the T_m value (~38.5°C), and broadened the temperature range of lipid melting, the effect of P_γ-FN being greater.

Fluorescence polarization

TMA-DPH was used to investigate the effects of the C-terminal Gγ peptides on the fluidity of the bilayer interface

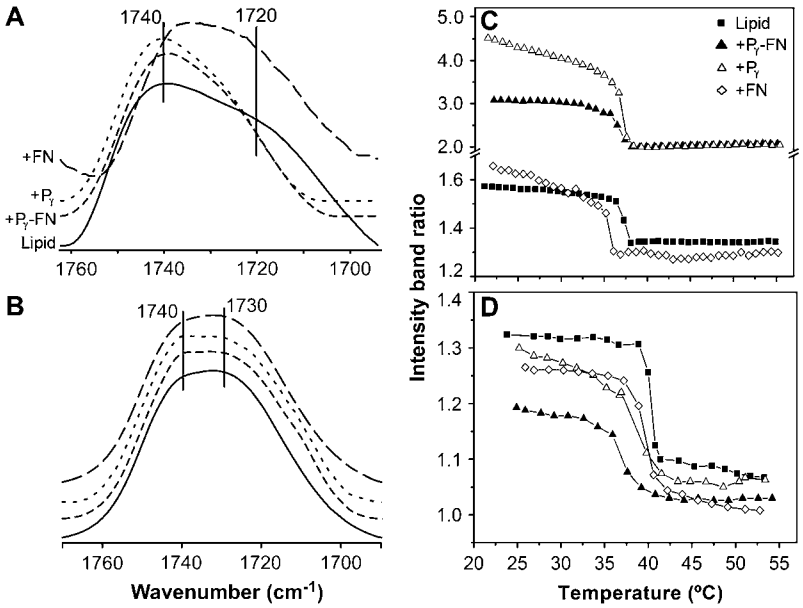

FIGURE 5 FTIR spectra of the C=O stretching mode region of DEPE and DMPS mixtures. (*A*) DEPE or (*B*) DMPS alone and in the presence of P_γ-FN, P_γ, or FN. The lipid/peptide or lipid/FN molar ratio was 10:1 in all cases. (*C* and *D*) Temperature profiles derived from the intensity band ratio of the deconvoluted CO stretching modes of DEPE or DMPS alone (■) and in the presence of P_γ-FN (▲), P_γ (△), or FN (◇).

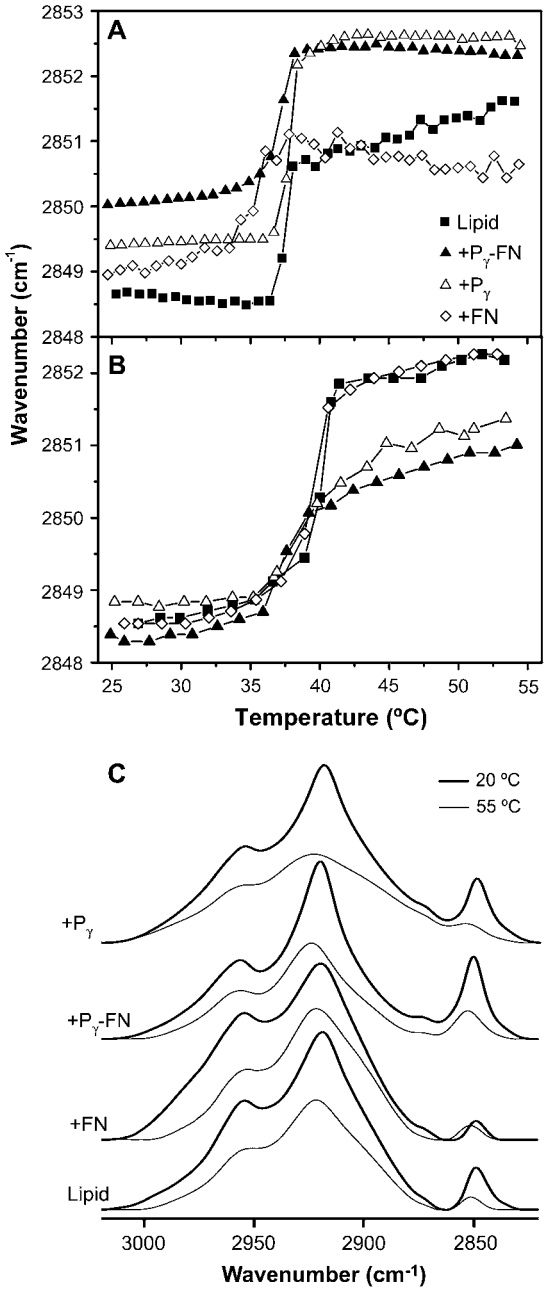

FIGURE 6 Temperature profiles of the CH_2 stretching band position. (*A*) DEPE or (*B*) DMPS alone (■) and in the presence of P_γ-FN (▲), P_γ (△), or FN (◇). The lipid/peptide or lipid/FN molar ratio was 10:1 in all cases. Similar results could also be obtained by plotting the data as the bandwidth at half-height instead of at the band position. (*C*) Illustration of temperature dependence for the C-H stretching region of the spectra of pure DEPE, 1:10 DEPE + FN, 1:10 DEPE + Pγ, 1:10 DEPE + Pγ-FN at 20°C and 55°C.

(Fig. 7). DEPE vesicles displayed a cooperative L_β-to-L_α phase transition ~35°C with an amplitude of ~22% (Fig. 7 *A*). In contrast to P_γ, both P_γ-FN and FN had similar effects on DEPE, provoking a decrease of the TMA-DPH fluorescence polarization and diminishing the transition amplitude (~11%–13%) in the L_β phase. However, neither P_γ-FN nor FN altered the fluorescence polarization of HPE-labeled DEPE liposomes in the lamellar phase temperature interval (data not shown), suggesting that neither of these compounds enters deeply into the acyl chain region of these PE bilayers. In DMPS membranes, the T_m value was ~37°C and the phase transition amplitude was ~41% (Fig. 7 *B*). By slightly increasing fluidity in the gel phase and decreasing it in the fluid phase, P_γ-FN decreased the T_m value and the amplitude of this transition in a concentration-dependent manner. In contrast, P_γ had only a modest effect on both parameters. Finally, DMPS membranes containing FN displayed similar properties to those with P_γ-FN, although FN did not change the magnitude of lipid polarization in the fluid phase.

DISCUSSION

In this study, we have shown that the C-terminal region of the Gγ subunit of G-proteins binds to model membranes through electrostatic and hydrophobic interactions driven by its amino acid and lipid moieties, respectively. This interaction induces changes in the membrane organization, which

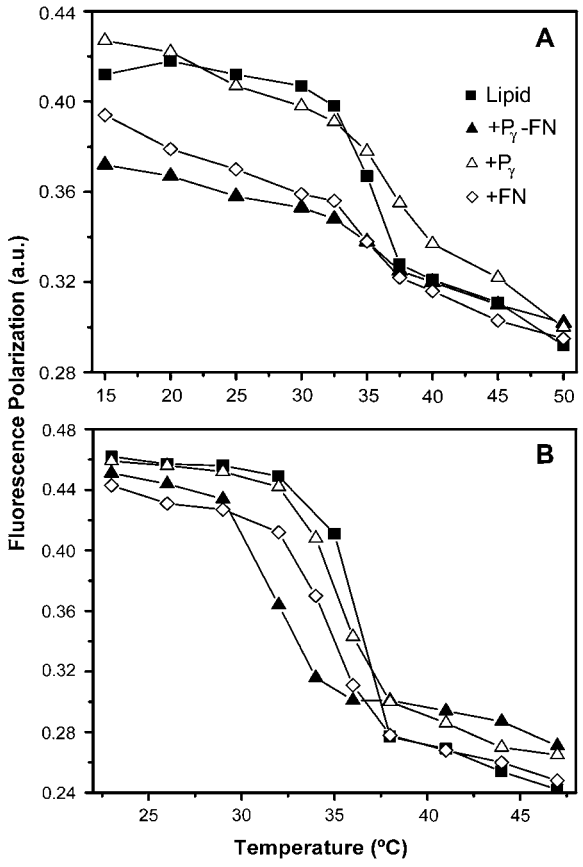

FIGURE 7 Fluorescence polarization of TMA-DPH-labeled DEPE and DMPS liposomes. Fluorescence polarization was measured in DEPE or DMPS membranes in the absence (■) or presence of P_γ-FN (▲), P_γ (△), or FN (◇). The lipid/peptide or lipid/FN molar ratio was 10:1 in all cases.

are relevant because they would favor a cooperative binding of G-proteins accounting in part for the high amounts of G-proteins found in certain regions rich in GPCRs (a molar excess of G-proteins over receptors is necessary for signal amplification). We have addressed a number of issues, first studying the effects of the peptide on membrane structure and then investigating the basis of the peptide-membrane interactions. Finally, we assessed the effects of membrane lipids on peptide structure. We found that the membrane binding of the C-terminal region of the $G\gamma_2$ protein was the result of various complex interactions. These included hydrophobic interactions between the FN group and membrane lipids that were favored by nonlamellar prone lipids (i.e., DEPE). Electrostatic interactions were also observed between the polar head of charged phospholipids (e.g., PS) and some positively charged amino acids of the $G\gamma_2$ protein, and these were more relevant than other hydrophilic interactions. In addition, membrane binding of P_γ-FN affected the structural organization of DEPE and DMPS model membranes, resulting in the formation of P_γ-FN-rich domains. The existence of such domains would partially explain the cooperative binding that characterizes the association of G-proteins with membrane lipids, facilitating the molar excess around G-protein-receptor clusters. Finally, membrane lipids had a modest effect on the structural properties of the peptide.

Effect of P_γ-FN on the lipid polymorphism of DEPE membranes

The effect of P_γ-FN was initially characterized by a modest stabilizing effect on the bilayer, increasing (by a few degrees) the L_α-to-H_{II} transition temperature. However, the nonlamellar phase propensity of membranes containing P_γ-FN was greater than that of DEPE membranes with P_γ only. This is in accordance with the fact that FN alone induces the formation of nonlamellar (H_{II}) phases (31). Additionally, the x-ray diffraction pattern of DEPE/P_γ-FN mixtures showed the presence of two nonlamellar H_{II} phases (H_{II}^a and H_{II}^b with $d = 6.5$ nm and 7.5 nm, respectively at 72°C) simultaneously. The domains associated with the smaller hexagonal lattice (H_{II}^a) are most likely poor in P_γ-FN since the lattice parameter varies in function of the temperature, like DEPE alone (23,31). The other domains (H_{II}^b) are most likely rich in P_γ-FN, as they showed little thermal lattice sensitivity but large thermal fluctuations. In cooling scans, the smaller hexagonal lattice H_{II}^a expanded until it reached the same dimensions of the larger hexagonal phase H_{II}^b. When the two hexagonal lattices reached a common dimension, a redistribution of the P_γ-FN over the lipid matrix surface took place during the formation of a single, therefore homogeneous, L_α phase. Moreover, DSC data also indicate that P_γ-FN segregates into peptide-rich and -poor domains, as the L_α-to-H_{II} transition peak could be resolved into two peaks. The calorimetric behavior shown was typical of nonhomogeneous mixtures and could explain intermolecular interactions of peptide molecules in peptide-rich domains associated with β-structures, as has been observed in FTIR studies.

In DEPE membranes, we previously found that FN segregated in the DEPE matrix, forming FN-rich and -poor domains (31). The former were associated with the formation of H_{II} phases at low temperature in the presence of lamellar domains. Here, DEPE/P_γ-FN membranes showed a different thermotropic behavior, probably due to the steric and electrostatic constraints inferred by the peptide moiety. Indeed, the H_{II} with a spacing of $d = 7.4$ nm (H_{II}^b) was not observed in DEPE alone or DEPE/P_γ mixtures, indicating that it must be associated with the presence of microdomains rich in P_γ-FN. It has been demonstrated that the FN group regulates the membrane curvature of PE membranes (40). The data shown here indicate that the FN moiety of P_γ-FN could be a structural determinant of nonlamellar phase propensity in a PE-rich environment.

Interaction of P_γ-FN with DMPS membranes

DSC endotherms of DMPS membranes displayed two peaks in the presence of P_γ-FN. This behavior reflects a nonhomogeneous mixture in which the peak with lower T_m corresponded to P_γ-FN-rich domains. The thermotropic behavior of the other peak was similar to that of DMPS alone and it decreased as the peptide concentration augmented, indicating that it was associated with P_γ-FN-poor domains. P_γ-FN-rich DMPS microdomains showed a thermotropic behavior similar to that of DMPS/FN mixtures. This result suggests that the FN moiety is involved in the association of the peptide with L_β phases and its later redistribution as the temperature increases. The lateral organization and phase when FN coexists in DMPC membranes has recently been described (41). However, the decrease in the calorimetric enthalpy observed in DMPS/P_γ-FN membranes (like DMPS/FN membranes) could be due to the hydrogen-bond network of the polar and interfacial regions of PS membranes (disrupted by the association of P_γ-FN, according to FTIR data) and the disordering induced by the insertion of the FN-group into the bilayer (as shown by fluorescence spectroscopy).

Molecular studies of P_γ-FN-lipid interactions

FTIR experiments demonstrated that the interaction of the C-terminal region of $G\gamma_2$ protein (P_γ-FN) with membranes mainly occurs at the polar and the interfacial regions of the lipid bilayer. Both P_γ-FN and P_γ form peptide-lipid complexes with the headgroup of acidic phospholipids. The spectral properties of the lipid phosphate group stretching modes in peptide/lipid mixtures were similar for both peptides, indicating that the peptide group moiety plays an active role in the peptide-lipid interaction at the polar region of the membrane lipid. In this interaction, the FN group of the peptide does not fulfill a relevant role, whereas the phosphate

group of the phospholipids appears to be directly involved. In fact, both peptides interact directly and induce a partial neutralization of these PO_2^{2-} groups. This association is most probably due to electrostatic binding and/or hydrogen bonding of the positively charged residues of the C-terminal region of the $G\gamma_2$ protein (33).

Additionally, P_γ-FN (like P_γ) also interacts with the interfacial region of the lipid bilayer through its peptide group, although certain differences were observed with the free peptide. In DEPE membranes, P_γ-FN produced significant dehydration and/or alteration of the hydrogen-bonded ester carbonyl groups in the L_β and L_α phases, favoring tighter lipid packing. The dehydration effect observed in DEPE membranes in the presence of P_γ-FN could favor the nonlamellar propensity observed (42). The binding of P_γ-FN also affected the acyl chain order of the lipid bilayer. P_γ-FN decreased the conformational order in DEPE membranes, although the CH_2 scissoring band was scarcely affected (data not shown). Considering the fluorescence spectroscopy data, this effect could be due to the FN group producing greater fluidity and a bigger contribution of the peptide moiety (more important in the L_α phase).

Although the FN chain can promote the appearance of H_{II} phases, our data show that the association of P_γ-FN with DEPE membranes modestly perturbed the hydrophobic region of the lipid bilayer. These results suggest that the positively charged amino acid residues on the C-terminus of the $G\gamma_2$ subunit interact with the interface of DEPE membranes, the FN moiety partially inserting into the bilayer. This relative position of the P_γ-FN in a DEPE membrane would increase the head/tail size ratio of DEPE molecules, decreasing the nonlamellar phase propensity compared to FN alone. As a consequence, the dimensions of the H_{II} phase (H_{II}^b) would enlarge as it is observed in the x-ray diffraction data. On the other hand, P_γ-FN increased the conformational order of DMPS acyl chains in the L_α phase. Whereas FTIR experiments could not elucidate whether the peptide binding induced lipid segregation, the results from x-ray diffraction and DSC experiments suggested the presence of peptide-rich and -poor domains. Despite the fact that both peptides P_γ-FN and P_γ had a similar effect on the DMPS bilayers, fluorescence polarization using TMA-DPH identified differences in these interactions. The FN moiety of P_γ-FN most likely increased the fluidity of the surface regions of the acyl chains, indicating that the FN group enters deeper into the membrane than P_γ. In addition, DSC experiments confirmed the interaction between FN and DMPS membranes.

It is noteworthy that in the P_γ-FN peptide (and the C-terminal region of $G\gamma_2$ protein) there are amino acid residues with a net positive charge. Since most of the positively charged residues of P_γ-FN are located close to the FN group, it is likely that the two Lys and the Arg residues (position 63, 64, and 61, respectively) establish electrostatic interactions with the charged moieties of the PS headgroups. These interactions would facilitate hydrogen bonding with the ester carbonyl groups in the interfacial region of the DMPS bilayer, as well as aiding in the docking of P_γ-FN (and the $G\gamma_2$ protein) and the insertion of the FN group into the membrane favoring a higher conformational order in the liquid phase as shown.

In summary, these experiments demonstrate that the binding of the C-terminal region of the $G\gamma_2$ protein to membranes involves: i), electrostatic interactions between the polar head and interfacial regions of phospholipids and the positively charged amino acids on the C-terminus of the $G\gamma_2$ protein; and ii), hydrophobic interactions between the FN moiety of the G-protein subunit and the fatty acyl residues of the lipids. Therefore, the lipid composition and structure of membranes play an important role in these interactions.

Biological significance

As well as studying the molecular basis of the binding of the C-terminal region of $G\gamma_2$ protein to model membranes containing lipids similar to those found by G-proteins in the plasma membrane, we also investigated the structural consequences of these interactions on both lipid and peptide structures. It was recently shown that prenyl groups facilitate the binding of G-protein $\beta\gamma$ complexes to membranes (9–11,43) and that the $G\beta\gamma$ dimer drives the interaction of G-proteins with H_{II}-prone membrane domains (rich in PE). In contrast, $G\alpha$-monomers prefer ordered lamellar regions (9). Moreover, the $G\gamma$ subunit is the closest to the lipid membrane (44). GPCRs are often clustered in defined membrane regions (45), and they can activate at least 20 G-protein molecules upon agonist activation. Therefore, the number of G-protein molecules in these membrane regions is very high, and the effect of prenyl groups on the lipid membrane structure and on the interactions between G-proteins and membrane lipids becomes particularly relevant. Our data in part explain the molecular mechanisms underlying the high density of G-proteins around these receptors. The transmembrane regions of membrane receptors increase the membrane nonlamellar phase propensity of membranes ((46) and references therein).

This facilitates G-protein binding to membranes (9,17), which further increases the nonlamellar phase propensity of membranes and the capacity to bind more G-proteins. Upon receptor activation, the G-protein $\beta\gamma$ complex remains associated with nonlamellar-prone regions whereas the α-subunit is recruited to ordered lamellar membrane regions (e.g., raft domains) where it interacts with signaling effectors to propagate incoming messages. Therefore, protein-lipid interactions play a pivotal role in cell signaling. In this context, our data reveal that the FN moiety of the $G\gamma$ subunit could be involved in the formation of G-protein clusters in membranes. The FN moiety would contribute to the H_{II} phase propensity. In membrane domains with high levels of PE and PS, the isoprenyl group favors the cooperative binding of G-proteins.

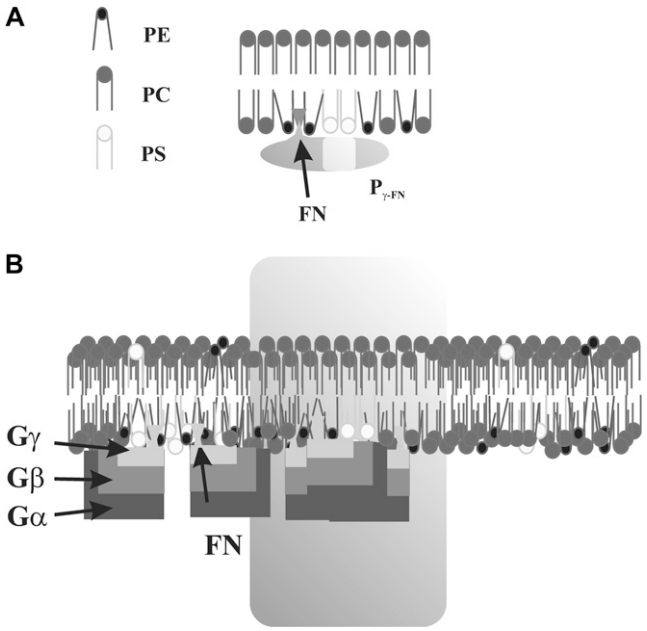

FIGURE 8 Schematic model for G-protein-membrane interactions. (*A*) Based on model membranes containing only one type of phospholipids molecule, this cartoon proposes that the P_{γ}-FN peptide binds to membranes through electrostatic interactions between its peptide moiety (*light gray*) and PS (*light gray*) and by hydrophobic interactions between the FN group (*triangle* in *dark color*) and PE (*black*). Phosphatidylcoline (PC) is shown in dark gray. (*B*) This panel shows the possible interaction of whole G-proteins with membranes, highlighting the role of the $G\gamma_2$ subunit. A membrane region with membrane receptors (R) and heterotrimeric G-proteins ($G\alpha\beta\gamma$) is shown. Both the transmembrane region of GPCRs and the FN moieties of G-proteins contribute to the nonlamellar phase propensity (31), which in turn favors the binding of G-proteins (9) and explains the cooperative interactions between these transducers and the regions with high PE content.

Along with earlier studies (9,17,19,20), these results suggest a model for G-protein-membrane interactions in which the association of these transducers with membranes is regulated by PS and PE and by the C-terminus of G-proteins (Fig. 8). It has recently been shown that PS is required for G-proteins to bind to membranes (20). In this context, the electrostatic interactions between the C-terminal region of the $G\gamma$ subunit and the PS residues indicate that this region of the G-protein is crucial for its interaction with the negatively charged phospholipid headgroups in the inner leaflet of the plasma membrane. There, the high levels of PE and PS indicate that their interaction with the FN moiety and the charged amino acids at the C-terminal region of the γ-subunit is an important component of the G-protein-membrane interaction. Thus, the membrane interaction of G-proteins regulates not only their localization but also their function (47,48).

This work was supported by the grants SAF2004-05249, BFU2005-00749, SAF2003-0032 (Ministerio de Educación y Ciencia, Spain), PRIB-2004-10131 (Govern Balear), I-02-066EC from Hamburger Synchrotrotron-strahlungslabor (Hamburg, Germany) by HPRI-CT-2001-00140 of the European Commission, The Marathon Foundation, and BANCAJA-UMH IP/UR/01.

REFERENCES

1. Casey, P. J. 1995. Protein lipidation in cell signaling. *Science*. 268: 221–225.
2. Sinensky, M. 2000. Functional aspects of polyisoprenoid protein substituents: roles in protein-protein interaction and trafficking. *Biochim. Biophys. Acta*. 1529:203–209.
3. Magee, T., and M. Hanley. 1988. Protein modification. Sticky fingers and CAAX boxes. *Nature*. 335:114–115.
4. Marshall, C. J. 1993. Protein prenylation: a mediator of protein-protein interactions. *Science*. 259:1865–1866.
5. Parish, C. A., and R. R. Rando. 1996. Isoprenylation/methylation of proteins enhances membrane association by a hydrophobic mechanism. *Biochemistry*. 35:8473–8477.
6. Niv, H., O. Gutman, Y. I. Henis, and Y. Kloog. 1999. Membrane interactions of a constitutively active GFP-Ki-Ras 4B and their role in signaling. Evidence from lateral mobility studies. *J. Biol. Chem*. 274: 1606–1613.
7. Moffett, S., D. A. Brown, and M. E. Linder. 2000. Lipid-dependent targeting of G proteins into rafts. *J. Biol. Chem*. 275:2191–2198.
8. Pereira-Leal, J. B., A. N. Hume, and M. C. Seabra. 2001. Prenylation of Rab GTPases: molecular mechanisms and involvement in genetic disease. *FEBS Lett*. 498:197–200.
9. Vogler, O., J. Casas, D. Capo, T. Nagy, G. Borchert, G. Martorell, and P. V. Escriba. 2004. The $G\beta\ \gamma$-dimer drives the interaction of heterotrimeric Gi proteins with nonlamellar membrane structures. *J. Biol. Chem*. 279:36540–36545.
10. Simonds, W. F., J. E. Butrynski, N. Gautam, C. G. Unson, and A. M. Spiegel. 1991. G-protein $\beta\ \gamma$ dimers. Membrane targeting requires subunit coexpression and intact γ C-A-A-X domain. *J. Biol. Chem*. 266:5363–5366.
11. Pronin, A. N., and N. Gautam. 1992. Interaction between G-protein β and γ subunit types is selective. *Proc. Natl. Acad. Sci. USA*. 89:6220–6224.
12. Sinensky, M. 2000. Recent advances in the study of prenylated proteins. *Biochim. Biophys. Acta*. 1484:93–106.
13. Fogg, V. C., I. Azpiazu, M. E. Linder, A. Smrcka, S. Scarlata, and N. Gautam. 2001. Role of the γ subunit prenyl moiety in G protein $\beta\ \gamma$ complex interaction with phospholipase Cβ. *J. Biol. Chem*. 276: 41797–41802.
14. Butrynski, J. E., T. L. Jones, P. S. Backlund Jr., and A. M. Spiegel. 1992. Differential isoprenylation of carboxy-terminal mutants of an inhibitory G-protein α-subunit: neither farnesylation nor geranylgeranylation is sufficient for membrane attachment. *Biochemistry*. 31: 8030–8035.
15. Kisselev, O. G., M. V. Ermolaeva, and N. Gautam. 1994. A farnesylated domain in the G protein γ subunit is a specific determinant of receptor coupling. *J. Biol. Chem*. 269:21399–21402.
16. Gudi, S., J. P. Nolan, and J. A. Frangos. 1998. Modulation of GTPase activity of G proteins by fluid shear stress and phospholipid composition. *Proc. Natl. Acad. Sci. USA*. 95:2515–2519.
17. Escriba, P. V., A. Ozaita, C. Ribas, A. Miralles, E. Fodor, T. Farkas, and J. A. Garcia-Sevilla. 1997. Role of lipid polymorphism in G protein-membrane interactions: nonlamellar-prone phospholipids and peripheral protein binding to membranes. *Proc. Natl. Acad. Sci. USA*. 94:11375–11380.
18. Matsuda, T., T. Takao, Y. Shimonishi, M. Murata, T. Asano, T. Yoshizawa, and Y. Fukada. 1994. Characterization of interactions between transducin $\alpha/\beta\ \gamma$-subunits and lipid membranes. *J. Biol. Chem*. 269:30358–30363.
19. Murray, D., S. McLaughlin, and B. Honig. 2001. The role of electrostatic interactions in the regulation of the membrane association of G protein $\beta\ \gamma$ heterodimers. *J. Biol. Chem*. 276:45153–45159.

20. Hessel, E., M. Heck, P. Muller, A. Herrmann, and K. P. Hofmann. 2003. Signal transduction in the visual cascade involves specific lipid-protein interactions. *J. Biol. Chem.* 278:22853–22860.

21. Ashby, M. N., D. S. King, and J. Rine. 1992. Endoproteolytic processing of a farnesylated peptide in vitro. *Proc. Natl. Acad. Sci. USA.* 89:4613–4617.

22. Surewicz, W. K., H. H. Mantsch, and D. Chapman. 1993. Determination of protein secondary structure by Fourier transform infrared spectroscopy: a critical assessment. *Biochemistry.* 32:389–394.

23. Funari, S. S., F. Barcelo, and P. V. Escriba. 2003. Effects of oleic acid and its congeners, elaidic and stearic acids, on the structural properties of phosphatidylethanolamine membranes. *J. Lipid Res.* 44:567–575.

24. Prades, J., S. S. Funari, P. V. Escriba, and F. Barcelo. 2003. Effects of unsaturated fatty acids and triacylglycerols on phosphatidylethanolamine membrane structure. *J. Lipid Res.* 44:1720–1727.

25. Kuhry, J. G., G. Duportail, C. Bronner, and G. Laustriat. 1985. Plasma membrane fluidity measurements on whole living cells by fluorescence anisotropy of trimethylammoniumdiphenylhexatriene. *Biochim. Biophys. Acta.* 845:60–67.

26. Lakowicz, J. R. 1999. Principles of Fluorescent Spectroscopy. Kluwer Academic/Plenium Publishers, New York. 291–320.

27. Casal, H. L., U. Kohler, and H. H. Mantsch. 1988. Structural and conformational changes of β-lactoglobulin B: an infrared spectroscopic study of the effect of pH and temperature. *Biochim. Biophys. Acta.* 957:11–20.

28. Demel, R. A., E. Goormaghtigh, and B. de Kruijff. 1990. Lipid and peptide specificities in signal peptide-lipid interactions in model membranes. *Biochim. Biophys. Acta.* 1027:155–162.

29. Lefevre, T., and M. Subirade. 2000. Interaction of β-lactoglobulin with phospholipid bilayers: a molecular level elucidation as revealed by infrared spectroscopy. *Int. J. Biol. Macromol.* 28:59–67.

30. Del Mar Martinez-Senac, M., J. Villalain, and J. C. Gomez-Fernandez. 1999. Structure of the Alzheimer β-amyloid peptide (25–35) and its interaction with negatively charged phospholipid vesicles. *Eur. J. Biochem.* 265:744–753.

31. Funari, S. S., J. Prades, P. V. Escriba, and F. Barcelo. 2005. Farnesol and geranylgeraniol modulate the structural properties of phosphatidylethanolamine model membranes. *Mol. Membr. Biol.* 22:303–311.

32. Desormeaux, A., G. Laroche, P. E. Bougis, and M. Pezolet. 1992. Characterization by infrared spectroscopy of the interaction of a cardiotoxin with phosphatidic acid and with binary mixtures of phosphatidic acid and phosphatidylcholine. *Biochemistry.* 31:12173–12182.

33. Nabet, A., J. M. Boggs, and M. Pezolet. 1994. Study by infrared spectroscopy of the interaction of bovine myelin basic protein with phosphatidic acid. *Biochemistry.* 33:14792–14799.

34. Pare, C., and M. Lafleur. 1998. Polymorphism of POPE/cholesterol system: a ^{2}H nuclear magnetic resonance and infrared spectroscopic investigation. *Biophys. J.* 74:899–909.

35. Hubner, W., H. H. Mantsch, F. Paltauf, and H. Hauser. 1994. Conformation of phosphatidylserine in bilayers as studied by Fourier transform infrared spectroscopy. *Biochemistry.* 33:320–326.

36. Mantsch, H. H., and R. N. McElhaney. 1991. Phospholipid phase transitions in model and biological membranes as studied by infrared spectroscopy. *Chem. Phys. Lipids.* 57:213–226.

37. Lewis, R. N. A. H., and R. N. McElhaney. 1996. Fourier transform infrared spectroscopy in the study of hydrated lipids and lipid bilayer membranes. *In* Infrared Spectroscopy of Biomolecules. H. H. Mantsch and D. Chapman, editors. Wiley-Liss, New York. 159–202.

38. Lewis, R. N., and R. N. McElhaney. 2000. Calorimetric and spectroscopic studies of the thermotropic phase behavior of lipid bilayer model membranes composed of a homologous series of linear saturated phosphatidylserines. *Biophys. J.* 79:2043–2055.

39. Zhang, Y. P., R. N. Lewis, R. S. Hodges, and R. N. McElhaney. 2001. Peptide models of the helical hydrophobic transmembrane segments of membrane proteins: interactions of acetyl-K2-(LA)12–K2-amide with phosphatidylethanolamine bilayer membranes. *Biochemistry.* 40:474–482.

40. Epand, R. F., C. B. Xue, S. H. Wang, F. Naider, J. M. Becker, and R. M. Epand. 1993. Role of prenylation in the interaction of the a-factor mating pheromone with phospholipid bilayers. *Biochemistry.* 32:8368–8373.

41. Rowat, A. C., D. Keller, and J. H. Ipsen. 2005. Effects of farnesol on the physical properties of DMPC membranes. *Biochim. Biophys. Acta.* 1713:29–39.

42. Lewis, R. N. A. H., D. A. Mannock, and R. N. McElhaney. 1997. Membrane lipid, molecular structure and polymorphism. *In* Lipid Polymorphism and Membrane Properties. R. Epand, editor. Academic Press, San Diego, CA. 25–102.

43. Takida, S., and P. B. Wedegaertner. 2003. Heterotrimer formation, together with isoprenylation, is required for plasma membrane targeting of Gβγ. *J. Biol. Chem.* 278:17284–17290.

44. Lambright, D. G., J. Sondek, A. Bohm, N. P. Skiba, H. E. Hamm, and P. B. Sigler. 1996. The 2.0 A crystal structure of a heterotrimeric G protein. *Nature.* 379:311–319.

45. Franco, R., V. Casado, F. Ciruela, J. Mallol, C. Lluis, and E. I. Canela. 1996. The cluster-arranged cooperative model: a model that accounts for the kinetics of binding to A1 adenosine receptors. *Biochemistry.* 35:3007–3015.

46. Escriba, P. V. 2006. Membrane-lipid therapy: a new approach in molecular medicine. *Trends Mol. Med.* 12:34–43.

47. Escriba, P. V., M. Sastre, and J. A. Garcia-Sevilla. 1995. Disruption of cellular signaling pathways by daunomycin through destabilization of nonlamellar membrane structures. *Proc. Natl. Acad. Sci. USA.* 92: 7595–7599.

48. Yang, Q., R. Alemany, J. Casas, K. Kitajka, S. M. Lanier, and P. V. Escriba. 2005. Influence of the membrane lipid structure on signal processing via G protein-coupled receptors. *Mol. Pharmacol.* 68:210–217.